JOURNAL OF GEOPHYSICAL RESEARCH, VOL. 117, D16304, doi:10.1029/2012JD017689, 2012

Validation of upper mesospheric and lower thermospheric temperatures measured by the Solar Occultation for Ice Experiment

Michael H. Stevens,[1] Lance E. Deaver,[2] Mark E. Hervig,[2] James M. Russell III,[3] David E. Siskind,[1] Patrick E. Sheese,[4] Edward J. Llewellyn,[5] Richard L. Gattinger,[5] Josef Höffner,[6] and B. T. Marshall[2]

Received 25 February 2012; revised 5 July 2012; accepted 5 July 2012; published 23 August 2012.

[1] Temperature observations in the polar mesosphere and lower thermosphere are critical for studies of polar mesospheric cloud (PMC) formation and variability. The Solar Occultation for Ice Experiment (SOFIE) on NASA's Aeronomy of Ice in the Mesosphere (AIM) satellite has been measuring temperatures in the polar atmosphere nearly continuously since 2007. We herein present an improved SOFIE temperature data set and validate it against a variety of satellite and ground-based observations. We find that when taking all comparisons together, SOFIE temperatures are in agreement with independent observations to within reported systematic uncertainties from 15 to 88 km altitude. Between 88 and 95 km SOFIE temperatures have a warm bias that peaks between 10 and 15 K in the Arctic summer and 20–30 K in the Antarctic summer. Much of the warm bias is likely related to uncertainties in prescribed atomic oxygen densities that are required for the SOFIE temperature retrieval.

Citation: Stevens, M. H., L. E. Deaver, M. E. Hervig, J. M. Russell III, D. E. Siskind, P. E. Sheese, E. J. Llewellyn, R. L. Gattinger, J. Höffner, and B. T. Marshall (2012), Validation of upper mesospheric and lower thermospheric temperatures measured by the Solar Occultation for Ice Experiment, *J. Geophys. Res.*, *117*, D16304, doi:10.1029/2012JD017689.

1. Introduction

[2] Since the first temperature measurements of the high latitude mesosphere in the early 1960s [*Theon et al.*, 1967; *Lübken*, 2000], there has been a great deal of interest in the cold summer mesopause and its relevance to the formation of polar mesospheric clouds (PMCs) [*von Zahn et al.*, 1996; *Berger and von Zahn*, 1999]. This is primarily because PMCs are extremely sensitive to the ambient temperature and could therefore be indicators of both natural and anthropogenic changes in the upper atmosphere.

[3] Accurate temperature profiles at high vertical resolution throughout the polar summer mesosphere are nonetheless still scarce. Temperature observations with the highest vertical resolution (≤1 km) can be obtained by either ground-based or in situ observations. Ground-based observations include those from potassium lidar [*Höffner and Lübken*, 2007; *Lübken et al.*, 2009] or iron (Fe) lidar [*Lautenbach and Höffner*, 2004]. In situ measurements at high vertical resolution (~0.2 km) can be obtained from sounding rockets [e.g., *Rapp et al.*, 2002] or at somewhat lower resolution (~3 km) from falling spheres [e.g., *Lübken et al.*, 1996; *Lübken and Müllemann*, 2003]. Summertime falling sphere observations have provided a clearer understanding of the seasonal evolution of the cold summer mesopause region [e.g., *Lübken*, 1999]. All of these ground-based temperature measurements are necessarily limited in geographical coverage, underscoring the need for complementary satellite temperature measurements to provide a more global-scale view.

[4] The Solar Occultation for Ice Experiment (SOFIE) on NASA's Aeronomy of Ice in the Mesosphere (AIM) satellite has measured temperature nearly continuously in the Arctic and Antarctic since May, 2007. SOFIE measures temperature and pressure using observations of atmospheric transmission in the 4.3 μm band of carbon dioxide (CO_2) and of atmospheric refraction in the 701 nm region [*Marshall et al.*, 2011] at a vertical resolution of 1–2 km. A discussion of the SOFIE experiment and some early results were presented by *Gordley et al.* [2009].

[5] Satellite temperature observations near the polar summer mesopause at sufficient vertical resolution (<5 km) for validation against SOFIE temperatures are relatively scarce. Three instruments that can provide these data are the Atmospheric Chemistry Experiment (ACE), the Sounding of the Atmosphere

[1]Space Science Division, Naval Research Laboratory, Washington, D. C., USA.
[2]GATS, Inc., Newport News, Virginia, USA.
[3]Center for Atmospheric Sciences, Hampton University, Hampton, Virginia, USA.
[4]Department of Physics, University of Toronto, Toronto, Ontario, Canada.
[5]Department of Physics and Engineering Physics, University of Saskatchewan, Saskatoon, Saskatchewan, Canada.
[6]Institute for Atmospheric Physics, Kühlungsborn, Germany.

Corresponding author: M. H. Stevens, Space Science Division, Naval Research Laboratory, Code 7641, 4555 Overlook Ave., SW, Washington, DC 20375, USA. (michael.stevens@nrl.navy.mil)

0148-0227/12/2012JD017689

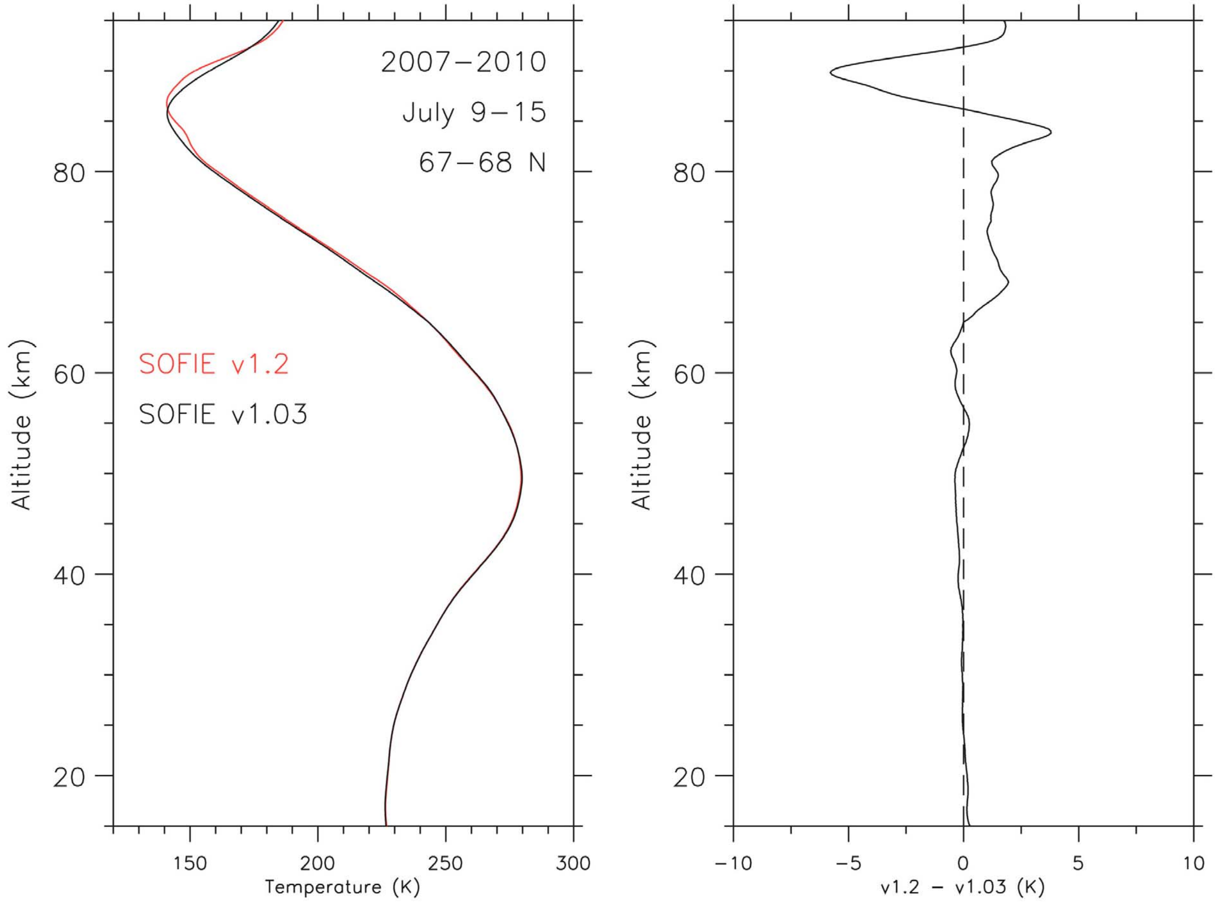

Figure 1. Comparison of SOFIE v1.03 and v1.2 temperatures in the Arctic summer. The profiles assembled for the indicated time and place are coincident with Arctic SABER temperature observations (see Figure 4).

using Broadband Emission Radiometry (SABER) and the Optical Spectrograph and Infrared Imaging System (OSIRIS). ACE provides gas phase temperature profiles throughout the PMC region using the technique of solar occultation [*Sica et al.*, 2008]. Its high inclination orbit (74°) allows for the simultaneous measurement of PMCs and temperature in the Arctic for about a week each July. SABER on NASA's Thermosphere, Ionosphere, Mesosphere, Energetics and Dynamics (TIMED) satellite retrieves kinetic temperature profiles in the Arctic mesosphere from the 15 μm band of CO_2 [*Remsberg et al.*, 2008]. SABER provides temperature profiles at latitudes up to 83° until about three weeks after summer solstice, at which time the satellite yaws so that SABER does not observe in the polar summer. Recently, *Sheese et al.* [2011a] reported polar summer temperatures measured by OSIRIS on the Odin Satellite. Using the rotational structure of the O_2 A-band, OSIRIS temperatures are reported at 88 km and above.

[6] We herein compare SOFIE temperature profiles to concurrent profiles from ACE, SABER and OSIRIS as well as ground-based Fe lidar profiles from 69°N. Our comparisons focus on the upper mesosphere and lower thermosphere in the Arctic and Antarctic during the summer. Particular attention is given to finding observations for data sets that are co-located in both space and time. Many previous studies that used earlier versions of the data have suggested a warm bias in SOFIE temperature retrievals in the upper mesosphere [e.g., *Hervig et al.*, 2009a; *Hervig and Gordley*, 2010; *Siskind et al.*, 2011]. This study will focus on where and when the SOFIE data agree with other measurements and where and when they do not.

[7] There are two objectives for the work presented here: (1) present recent improvements to SOFIE temperature retrievals resulting in the latest publicly released Version 1.2 (v1.2) data set, and (2) compare SOFIE v1.2 temperature profiles against a variety of satellite and ground-based measurements to validate the new retrievals. This work is arranged as follows: in section 2 we discuss the SOFIE data set and the measurement geometry. In section 3 we provide details on the new SOFIE temperature retrievals and discuss differences with the previous publicly released version (v1.03). In section 4 we compare SOFIE temperature observations to other satellite and ground-based observations and

Table 1. SOFIE Temperature Uncertainties in the Polar Summer

Altitude (km)	Precision–One Scan (K)	O Profile (K)	CO_2 Profile (K)	Total[a] (K)
80	0.1	0.0	0.8	0.8
85	0.2	0.4	2.1	2.1
90	0.2	0.7	5.6	5.6
95	0.5	7.3	6.7	9.9

[a]Quadratic sum of O and CO_2 uncertainty.

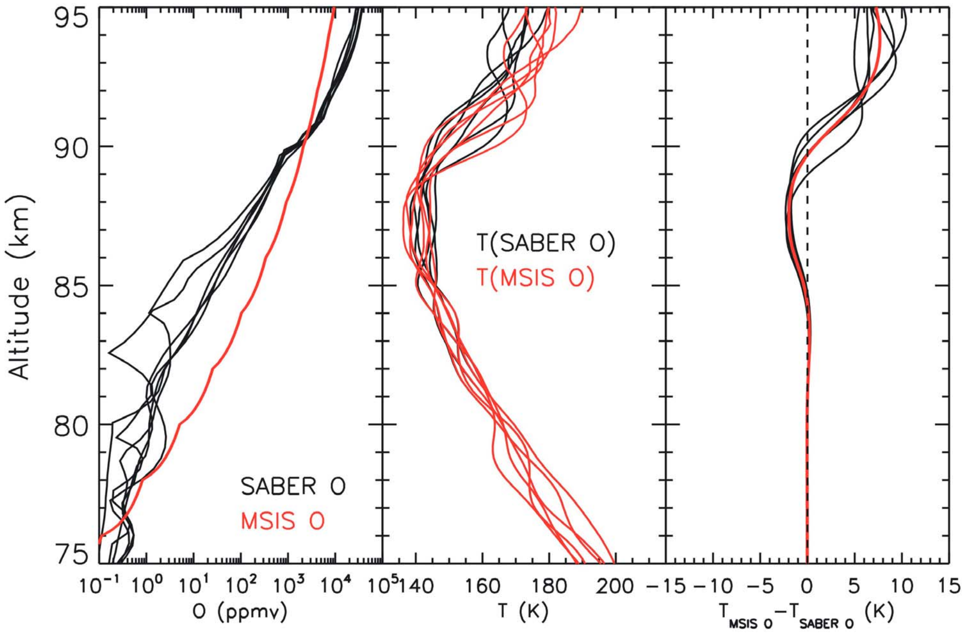

Figure 2. (left) Six SABER atomic oxygen (O) profiles in black obtained simultaneously with SOFIE observations on 10 July 2010. MSIS O profiles used in the SOFIE temperature retrievals are shown in red. (middle) SOFIE retrieved temperatures using SABER O (black) and NRLMSISE-00 O (red). (right) Difference between SOFIE retrievals using NRLMSISE-00 O and SABER O. The average is shown in red.

in section 5 we summarize the results and offer possible explanations for any differences.

2. The SOFIE Observations

[8] The AIM satellite was launched on 25 April, 2007 into a nearly circular sun-synchronous retrograde orbit with an inclination of 97.4° [*Russell et al.*, 2009]. SOFIE observes 15 solar occultations in the northern hemisphere and 15 in the southern hemisphere each day at latitudes between 66° (at solstice) and 83° (at equinox) [*Marshall et al.*, 2011]. The local time (LT) at the tangent point for each of the occultations is nearly constant at 23:00 in the northern hemisphere and 01:30 in the southern hemisphere. SOFIE obtains temperature profiles between 15 km and 95 km in both hemispheres and continues to take data without significant interruption.

[9] In this study we will focus primarily on the altitude region between 75 and 95 km, since this is the altitude region most relevant to PMC studies and the AIM science objectives. Temperatures measured by SOFIE were reported in many previous studies using earlier versions of the data [e.g., *Hervig et al.*, 2009a, 2009b; *Gordley et al.*, 2009; *Russell et al.*, 2009; *Hervig and Gordley*, 2010; *Russell et al.*, 2010: *Marshall et al.*, 2011; *Sheese et al.*, 2011a; *Siskind et al.*, 2011]. Most of these studies indicated that the SOFIE temperatures contained a warm bias of 7 K or more near the mesopause. The new v1.2 SOFIE temperature retrievals improve on the v1.03 retrievals in many aspects discussed below. The v1.2 temperatures have not been validated against any independent and concurrent measurements heretofore.

3. The SOFIE Version 1.2 Temperature Retrievals

[10] SOFIE temperature retrievals above 50 km use broadband transmittance measurements in the 4.3 μm absorption band of CO_2. A detailed description of the SOFIE temperature retrieval procedure including sensitivity studies and error analysis is found in *Marshall et al.* [2011] so we herein only discuss recent improvements in the v1.2 algorithm. These improvements can be categorized by field of view (FOV) corrections affecting the forward model and adjustments to the prescribed CO_2 and atomic oxygen (O) profiles required for the retrievals. They are discussed in order below.

[11] The SOFIE Level 1 algorithm assigns latitude and longitude to the occultation event, corrects the signals for instrument effects, and registers the signals in altitude and pressure. The v1.2 data presented herein include a better characterization of the FOV wings from analyzing data collected during scans of the solar disk. The new FOV analysis provides a more accurate altitude registration and improves the forward model by accounting for both the vertical gradient in transmission and the variation in solar intensity across the disk. In addition, new emissivity tables for the broadband CO_2 channels were computed on a finer vertical grid, which improves the accuracy of the forward model.

[12] As discussed in *Marshall et al.* [2011], SOFIE provides high quality results under the premise that the atmospheric CO_2 and O profiles are well known. In the stratosphere the CO_2 mixing ratio is near constant, however above about 80 km molecular diffusion becomes important and the mixing ratios decrease. It is in this region where uncertainties in our knowledge of the CO_2 vertical profile are largest. Also, in this altitude region the radiative transfer model must account for a CO_2 vibrational state distribution that is no longer determined strictly from local thermodynamic equilibrium (LTE) processes, and quenching by O must therefore be considered. This is particularly important in the vicinity of the polar summer mesopause and the lower thermosphere.

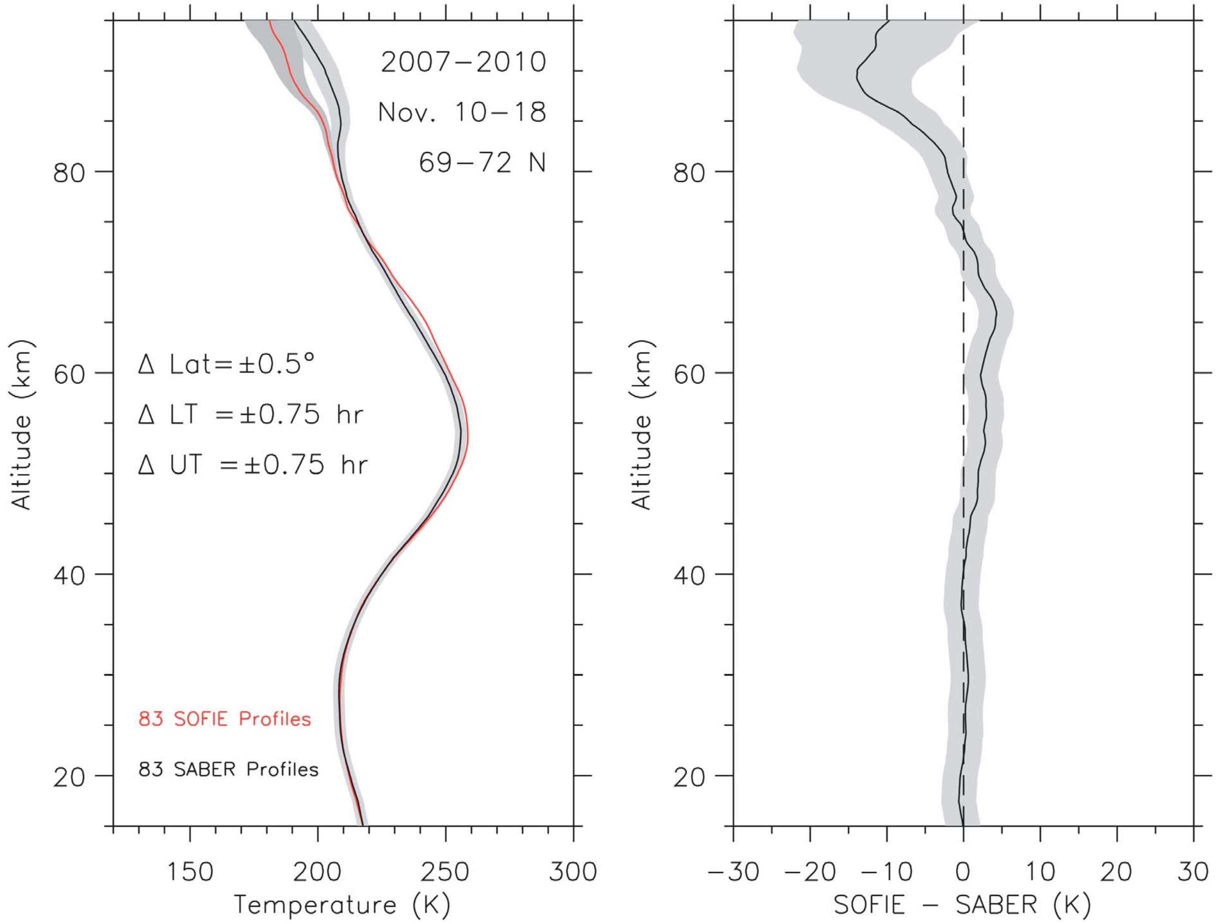

Figure 3. (left) Comparison of SOFIE v1.2 temperature profiles with coincident SABER profiles in November. The pairs of profiles selected for comparison all fall within the indicated window of latitude, LT and UT and are assembled from four years of data. Temperature uncertainties for each average profile are indicated by the shaded areas. (right) The difference between the two averages, where the shaded area indicates the quadratic sum of the temperature uncertainties for SABER [*Remsberg et al.*, 2008] and SOFIE.

[13] The SOFIE v1.03 temperature retrieval algorithm had an error that led to the forward model using incorrect CO_2 and O mixing ratio profiles, which has been corrected in v1.2. For v1.2 we have also made adjustments to several rate constants to make them consistent with values used in the SABER non-LTE algorithm. The non-LTE effects for SOFIE are explicitly modeled using the CO_2 non-LTE models developed for SABER [*López-Puertas and Taylor*, 2001; *Mertens et al.*, 2001; *Kutepov et al.*, 2006]. Note that the lower energy states of CO_2 are relevant for the SOFIE 4.3 μm band in occultation whereas the upper energy states are relevant for the emission measurement of the SABER 15 μm band.

[14] The improvements discussed above have resulted in significant changes in the retrieved temperature profiles for v1.2. For both v1.03 and v1.2 the SOFIE temperature retrievals extend up to 102 km, so that the approximations used at the top of the retrievals have negligible impact to the temperatures below 95 km shown herein. The difference between v1.2 and v1.03 temperatures in the Arctic summer is shown in Figure 1, where the temperatures at 90 km are now reduced by 6 K in v1.2 compared to v1.03. We also note from Figure 1 that temperatures near the PMC altitude of 83 km are warmer compared to v1.03 by 4 K.

[15] In order to better characterize the sensitivity of the SOFIE retrieval to the prescribed CO_2 and O profiles, we estimate the uncertainties in the retrieved temperatures due to these important inputs and summarize the results in Table 1. The SOFIE v1.2 algorithm (as in all previous versions) makes use of the O profile calculated from the NRLMSISE-00 empirical model [*Picone et al.*, 2002]. The scans assembled in Figure 1 are coincident with SABER scans both temporally and spatially (see section 4) so we have compared six of these retrieved temperature profiles using the NRLMSISE-00 O profiles and SABER O profiles and these results are shown in Figure 2. We find in all cases analyzed, the SABER O profiles reduce the SOFIE temperature between 90 and 95 km. The effect is largest at 95 km where the temperature is 7 K less and the SABER O is about a factor of two to three larger than NRLMSISE-00. We emphasize that comparisons of SABER O profiles to other measurements and empirical models in this altitude region indicate that SABER O is larger by factors of 2–5 [*Smith et al.*, 2010], which is greater than the O differences tested

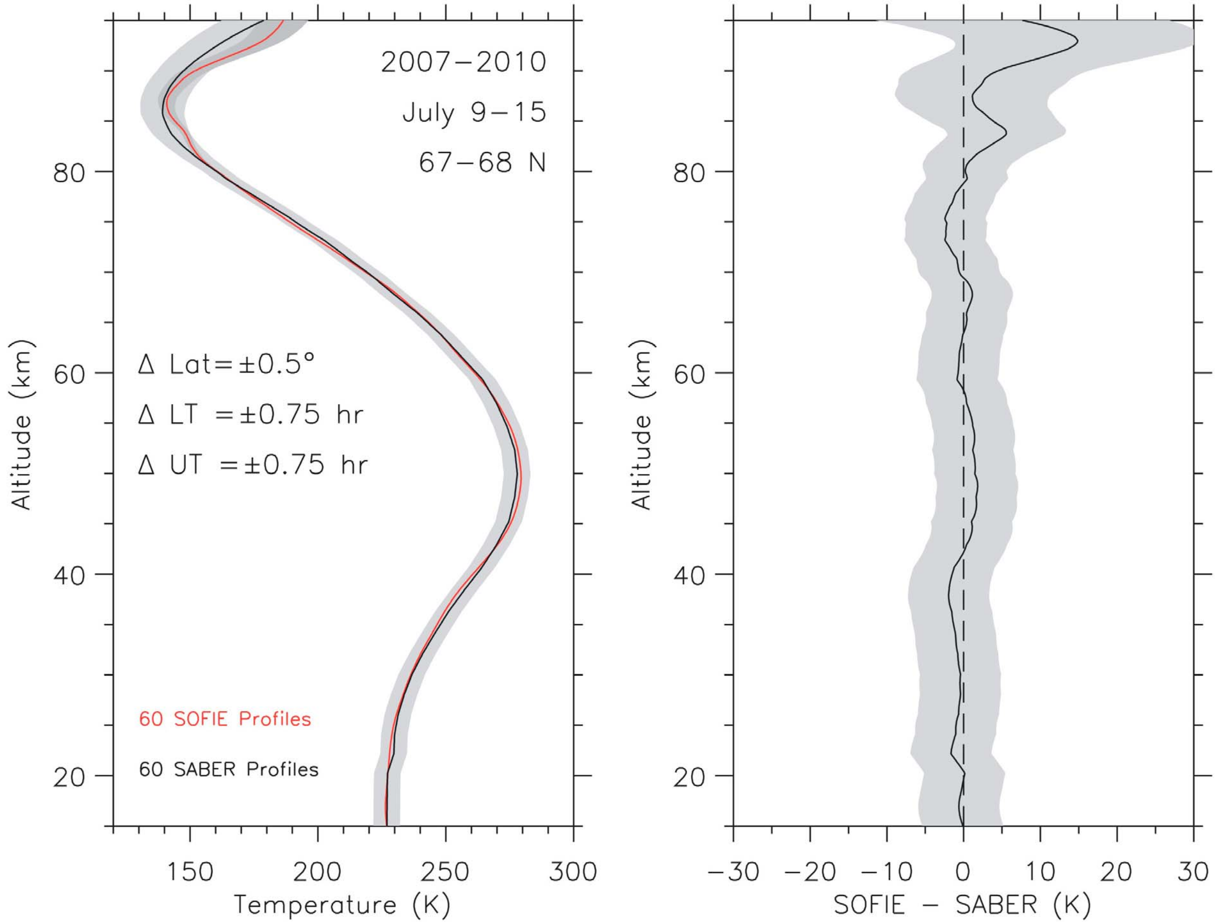

Figure 4. (left) Comparison of SOFIE temperature profiles with coincident SABER profiles in July and (right) difference between the profiles. The profiles selected for comparison all fall within the indicated window of latitude, LT and UT. The shaded region in Figure 4 (right) represents the combined uncertainties of the two data sets.

here. Moreover, *Sheese et al.* [2011b] found OSIRIS derived O densities in the Arctic summer mesopause region are typically larger than NRLMSISE-00 O densities by factors of five to ten and seasonal oscillations of O out of phase with NRLMSISE-00 O by six months. The determination of O densities in this altitude region is beyond the scope of this paper but it is clearly important to the retrieval of SOFIE temperatures between 85 and 95 km.

[16] SOFIE v1.2 temperature retrievals, like all previous versions, use CO_2 mixing ratio profiles from a climatology developed from the Whole Atmosphere Community Climate Model [*Garcia et al.*, 2007]. Using the sensitivity study of *Marshall et al.* [2011], we find that a 15% uncertainty in the CO_2 mixing ratio at 95 km results in a 7 K uncertainty in temperature at that altitude.

4. Comparison With Concurrent Observations

[17] We now compare SOFIE mesospheric temperature profiles against results from three different satellite experiments observing during the Arctic summers of 2007–2010: ACE (version 3.0), SABER (version 2.00) and OSIRIS. We select the profiles from each data set that are as close as possible in LT, latitude, and UT to the SOFIE observations so as to minimize differences due to tides, latitudinal temperature gradients and temporal variations including the effects of planetary waves. We also collect as many profiles as possible from each data set to minimize the statistical uncertainty and to obtain a representative average from the observed geophysical variability of the temperature profiles.

[18] We divide the comparisons into three sections based on the season and location of the observations. In section 4.1 we compare SOFIE temperatures in the northern hemisphere to SABER observations outside of the PMC season in November. In section 4.2 we compare SOFIE temperatures in the Arctic summer to SABER, ACE and OSIRIS observations as well as ground-based Fe lidar observations. Finally, in section 4.3 we compare SOFIE temperatures in the Antarctic summer to SABER and ACE observations.

4.1. Arctic Autumn Temperatures

[19] The SABER observations precess in LT so that coincident observations with SOFIE are limited to specific days of the year when the fixed LT of the SOFIE measurements is the same as SABER. In mid-November there are a few days during which SABER and SOFIE are measuring nearly the

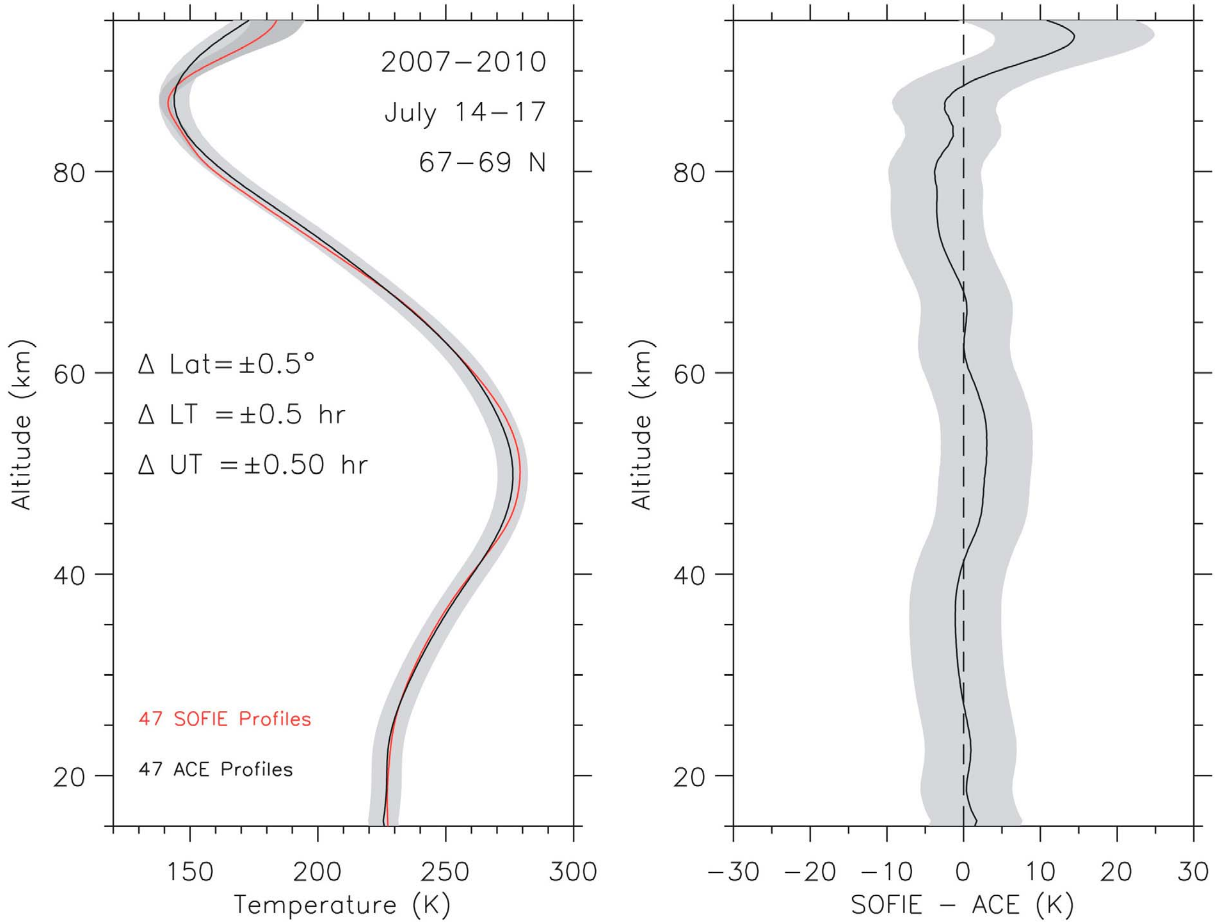

Figure 5. (left) Comparison of SOFIE temperature profiles with coincident ACE profiles in July. The overplotted red curve shows the SOFIE profile smoothed over the 4 km vertical resolution of the ACE measurements. The selected profiles for comparison were found within the indicated constrains of latitude, LT and UT. The difference is shown to the right with the indicated uncertainty a quadratic sum of the SOFIE systematic uncertainty and the ACE uncertainty of 6 K [*Sica et al.*, 2008]. (right) The smoothed SOFIE profile is compared against the ACE average.

same parcels of air at the same time. Figure 3 shows a comparison of SOFIE temperatures with concurrent SABER temperature observations from 15 to 95 km. The miss distance in latitude and the time differences are indicated and small enough so that each SOFIE scan used is paired with a single SABER scan.

[20] The SABER data used in these comparisons are from a preliminary version of the next production release v2.0. These data differ from version 1.07 due to refinement of the off-axis field of view (FOV) functions and changes to the forward model, of which the most important is the O volume mixing ratio (VMR) profile used in the vibrational temperature model. These differences are typically less than 2 K below 80 km but may exceed 5 K above, particularly for the upper mesosphere and lower thermosphere during polar summer and polar winter. The SABER data used in these comparisons is expected to be within 1 K of publicly released v2.0 data below the middle mesosphere and within 5 K in the upper mesosphere and lower thermosphere. Details on the SABER temperatures will be provided in a forthcoming publication.

[21] The vertical resolution of the SABER temperature retrievals is ~2 km [*Remsberg et al.*, 2008], which is close to the resolution of the SOFIE retrievals [*Hervig et al.*, 2009a]. SABER systematic temperature uncertainties are taken from *Remsberg et al.* [2008]. Random temperature uncertainties of both SABER and SOFIE for the average comparisons in Figure 3 and all future satellite intercomparisons herein are less than 1 K and not included (see Table 1). The right hand panel shows the difference between the two averaged profiles and the agreement is very good below 75 km. Between 75 and 95 km SOFIE is colder than SABER by 10–15 K, however this is nearly within the combined uncertainty of the two instruments. The combined uncertainty shown as the shaded region in the right hand panel is the quadratic sum of the total SOFIE systematic uncertainty (Table 1) and the total SABER systematic uncertainty [*Remsberg et al.*, 2008].

4.2. Arctic Summer Temperatures

[22] The polar summer mesosphere is the primary region of scientific interest for the AIM mission so we focus on this

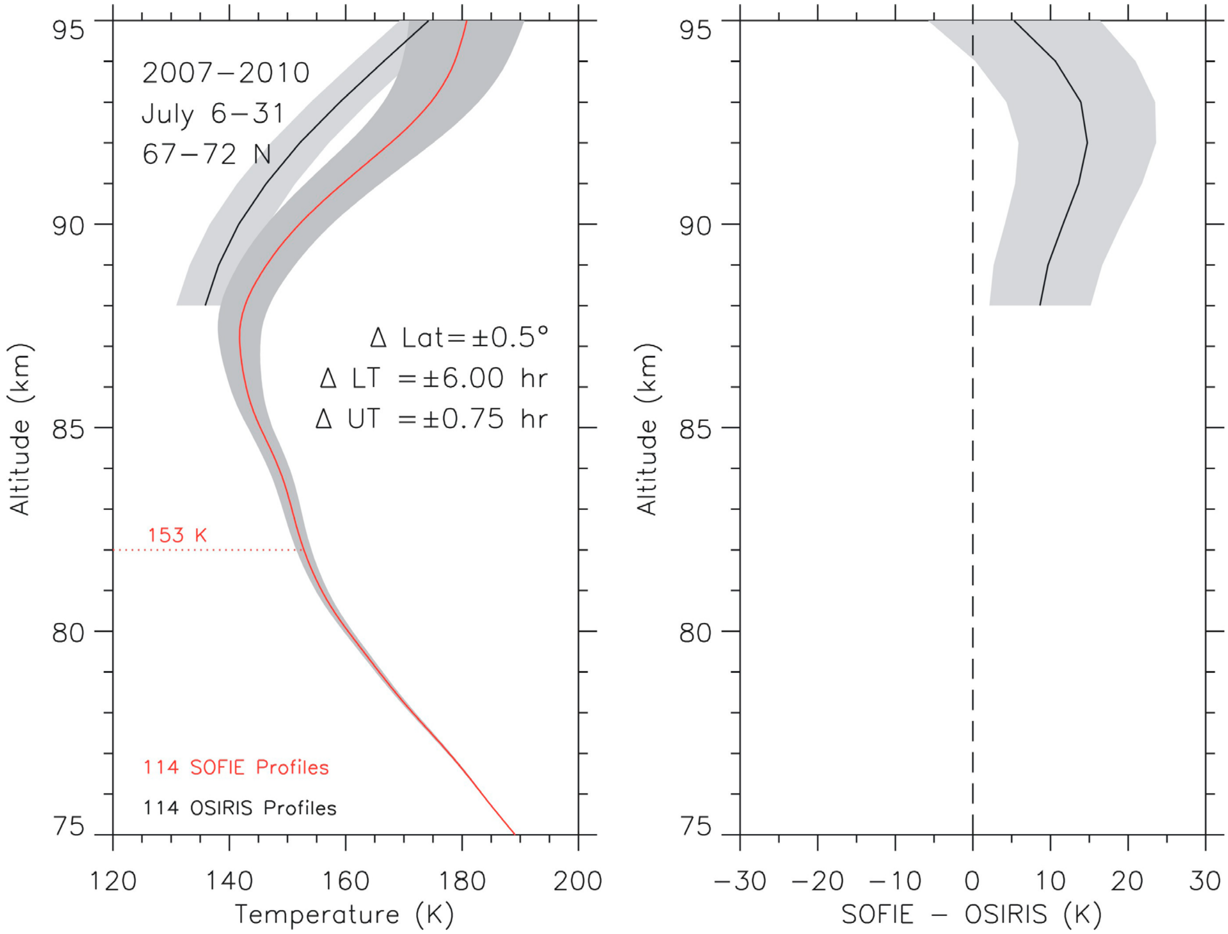

Figure 6. (left) Comparison of SOFIE temperature profiles with coincident OSIRIS profiles in July. Profiles were found within the indicated constrains of latitude, LT and UT. (right) The difference is shown with the indicated uncertainty a quadratic sum of the SOFIE systematic uncertainty and the OSIRIS uncertainty.

region for the rest of our analysis. We compare SOFIE temperatures observed during the Arctic summer to three different sets of satellite observations and one set of ground-based observations from 69°N. Figure 4 shows SOFIE temperatures compared to SABER temperatures from 15 to 95 km altitude from July, 2007–2010. The agreement is exceptionally good and within reported combined systematic uncertainties at all altitudes. We note that the SABER systematic temperature uncertainty is larger in the polar summer than in November (Figure 3) [*Remsberg et al.*, 2008]. The geophysical variability observed by SOFIE for one scan is about 5 K at 80 km and 10 K at 90 km [*Marshall et al.*, 2011]. In Figure 4 (right) we show the difference between the two profiles and there is a suggestion that SOFIE temperatures are systematically warmer than SABER temperatures by about 10–15 K between 90 and 95 km altitude, but this is still within the combined uncertainty of the two experiments. This apparent warm bias in the SOFIE temperatures is clarified further in comparisons with the ACE experiment.

[23] Figure 5 shows a comparison of SOFIE and ACE temperature profiles from July 14–17 assembled for the four years between 2007 and 2010. The ACE temperature retrievals have a vertical resolution of about 4 km [*Petelina and Zasetsky*, 2009] so we smooth the average SOFIE profile by this amount prior to comparison with ACE. The agreement is remarkably good for all altitudes from 15 km up to 90 km and within the combined systematic uncertainty of the two experiments. Between 90 and 95 km the difference in the right hand panel shows that SOFIE temperatures are systematically warmer than the ACE temperatures by 10–15 K. These results are therefore very similar to those from SABER in Figure 4.

[24] Figure 6 shows a comparison of SOFIE and OSIRIS July temperatures in the Arctic between 2007 and 2010. We note here that OSIRIS is in a sun-synchronous orbit like SOFIE, however the LT sampled by the two instruments are quite different. The OSIRIS observations closest in time to the SOFIE observations are on the ascending node of the Odin orbit near 17:30 LT and we make no attempt here to remove any effects due to the influence of tides. OSIRIS temperatures are reported at and above 88 km [*Sheese et al.*, 2011a] and the difference shown in the right hand panel indicates that SOFIE is warmer than OSIRIS by up to 10–15 K between 88 and 95 km, also consistent with SABER and ACE results. The absolute OSIRIS temperature uncertainty used in Figure 6 is 5 K and constant with altitude. We note that the SOFIE temperature near PMC altitudes (82 km) of 153 K is consistent with temperatures reported from a

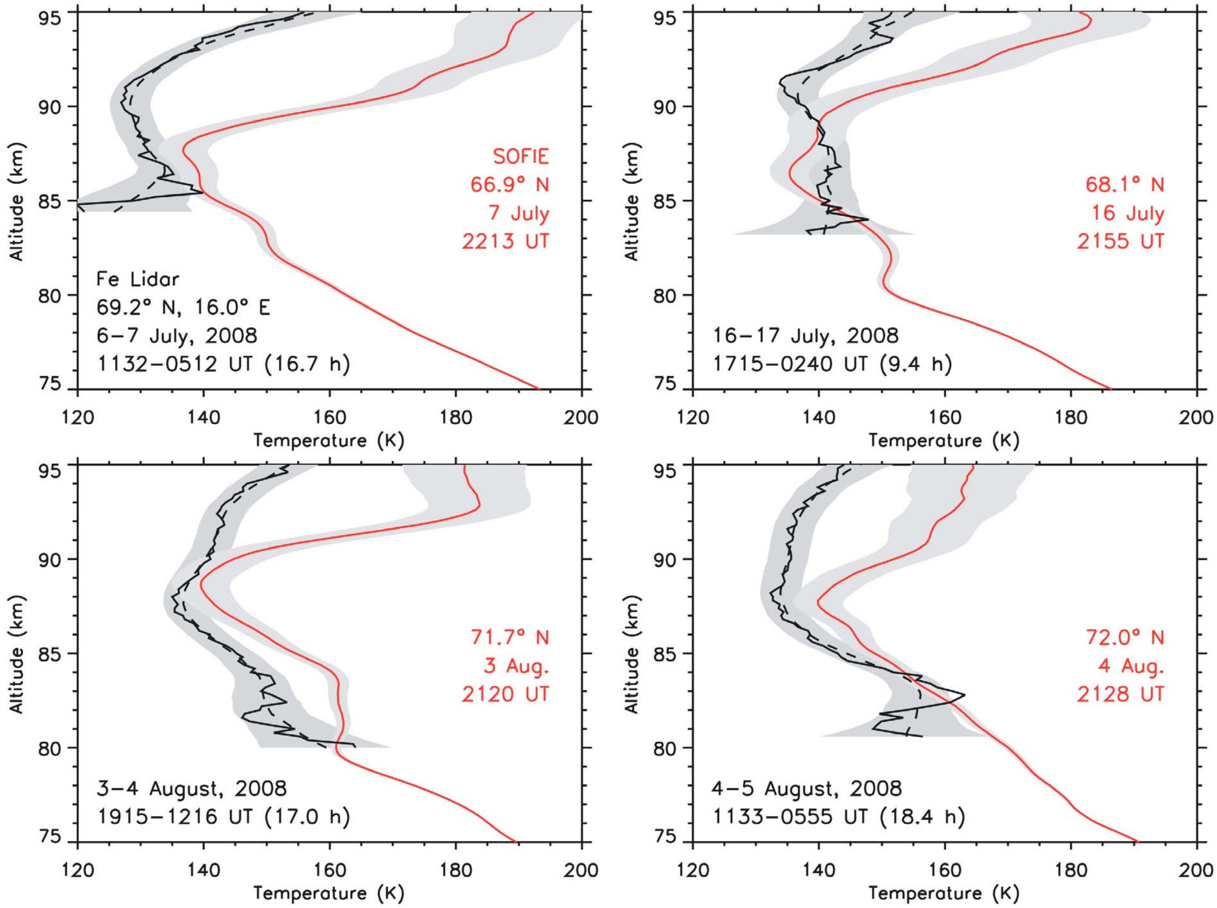

Figure 7. Comparison of Fe lidar temperature measurements at 69°N in 2008 (black) with SOFIE temperatures (red). The dashed line is the Fe lidar profile smoothed to the vertical resolution of SOFIE. There are four different time periods in July and August indicated and the SOFIE profile is the nearest to the ground-based measurement in space and time. UT over which the Fe lidar profile is averaged is indicated as well as the total amount of time for the average in parentheses. Shaded envelopes show the uncertainty of the measurements. The Fe lidar uncertainty is a combination of the statistical and the systematic contributions.

climatology of falling sphere observations observed at the same latitude for late July conditions (149 ± 4 K) [*Lübken*, 1999].

[25] Finally, in Figure 7 we compare the SOFIE temperature measurements directly with ground-based measurements of a Fe lidar that was making observations from ALOMAR (69°N) during the 2008 summer. We emphasize that such comparisons between ground-based and satellite observations implicitly contain differences not present in the satellite comparisons shown above. Specifically, the ground-based data are averaged over 9–19 h so that tidally induced variations of temperature are generally averaged out whereas SOFIE is always measuring at a specific LT. In addition, because SOFIE scans the limb of the Earth, the SOFIE observations are smoothed horizontally over about 290 km whereas the ground-based data are measuring at one geographical point and can offer considerably better vertical resolution.

[26] Nonetheless we smooth the Fe lidar temperatures with the 1.5 km vertical resolution of SOFIE and show comparisons during four different time periods in July and August, 2008 in Figure 7. The averaged Fe lidar temperature profiles are compared against single SOFIE temperature profiles closest in space and time to the Fe lidar observations. Figure 8 shows the differences between these profiles and in general there is agreement up to about 88 km but between 88 and 95 km the SOFIE profiles are again systematically warmer than the Fe lidar averaged profiles. The difference is between 20 and 50 K and larger than those from the satellite profiles, although the differences in the observational techniques stated above may contribute to this disagreement.

4.3. Antarctic Summer Temperatures

[27] We consider the same three satellite data sets for a comparison of temperatures in the Antarctic summer. Figure 9 shows a comparison between SOFIE and SABER temperature observations in late December and early January for the three years 2008–2010. Here we emphasize again that the SABER temperatures are a new version that will be the next public release of data. As is the case for the Arctic summer, the agreement with SABER temperatures in the Antarctic summer is excellent up to 90 km. SOFIE temperatures are higher between 90 and 95 km by 20–25 K,

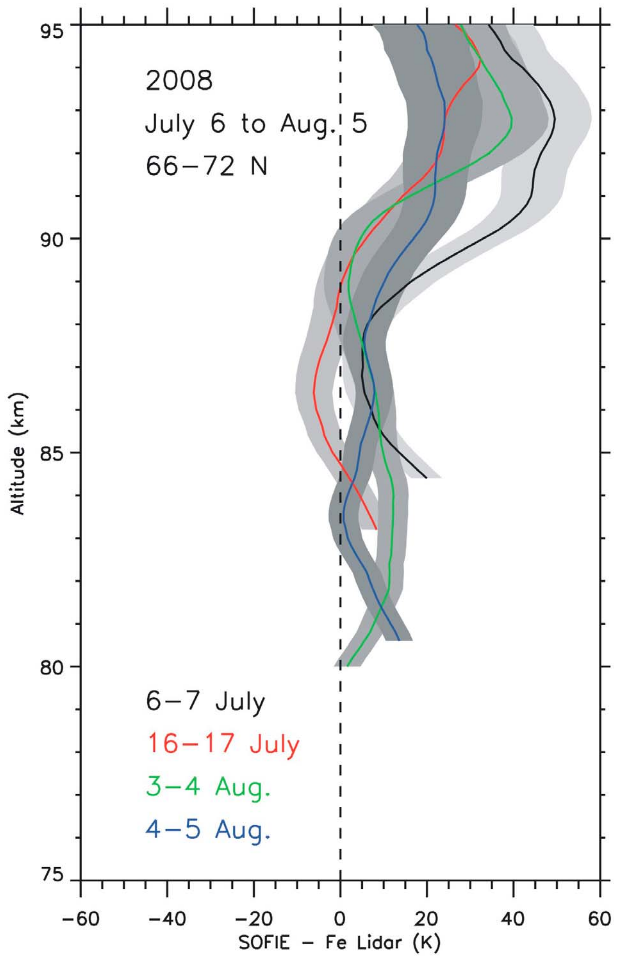

Figure 8. Difference of the SOFIE and Fe lidar profiles shown in Figure 7. Shaded area represents the quadratic sum of the two sets of uncertainties in the Fe lidar profile and the SOFIE profile.

which is larger than the warm bias seen in the Arctic summer at the same altitudes.

[28] Figure 10 shows a comparison between SOFIE and ACE temperatures for the time period between 9 and 10 January during the years 2008–2010. The agreement is within the uncertainties up to ~87 km and above that the warm bias of the SOFIE temperatures appears once again, peaking between 25 and 30 K near 93 km altitude.

[29] Figure 11 shows a comparison between SOFIE and OSIRIS temperatures from January, 2008–2010. For these southern hemisphere observations we assemble the OSIRIS data from the descending node of the Odin orbit near 07:00 LT, which is closest to the SOFIE observations near 01:30 LT. Note that at 82 km the SOFIE temperatures are 6 K warmer than in the Arctic summer, with the average at 159 K. This SOFIE temperature of 159 K is also 7 K warmer than that reported from falling sphere measurements obtained in 1998 at Rothera, Antarctica (152 ± 4 K) [*Lübken et al.*, 2004]. Above 88 km, SOFIE is again systematically warmer than OSIRIS with a peak of about 30 K at 92–93 km. Taken together, Figures 9–11 show that the SOFIE warm bias between 90 and 95 km altitude is about twice as large (20–30 K) in the Antarctic summer compared to the Arctic summer (10–15 K).

5. Discussion and Summary

[30] We find that contrary to previous work using earlier versions of SOFIE data, there is no warm bias for SOFIE temperatures in the polar summer up to 88 km within the uncertainties of independent satellite data sets (SABER, ACE and OSIRIS). This agreement is consistently found in the Arctic autumn, the Arctic summer and the Antarctic summer and is best when using measurements of SABER and ACE, which can observe at the same local time as SOFIE. The agreement exists in spite of the fact that SOFIE v1.2 temperatures are up to 3 K greater at PMC altitudes than the last publicly released version of SOFIE temperatures (v1.03) in the Arctic summer (Figure 1).

[31] Between 88 and 95 km there is evidence for a systematic warm bias in the SOFIE temperatures that is persistently found in comparison with all data sets in the polar summer, including ground-based Fe lidar observations. This warm bias peaks near 93 km and is between 10 and 50 K in the Arctic summer, but for the satellite data with profiles co-located in space and time this difference is less and between 10 and 15 K. In the Antarctic summer this warm bias occurs at the same altitude but it is larger and between 20 and 30 K.

[32] Because of the hemispheric difference in the bias between 88 and 95 km, it is unlikely that it arises solely from uncertainties in prescribed reaction rates required for the SOFIE non-LTE retrieval. Moreover, the SABER temperature retrieval and the SOFIE temperature retrieval use the same CO_2 climatology [*Garcia et al.*, 2007], so it is unlikely that this is the primary source of the warm bias in the polar summer since SABER shows a similar bias in SOFIE temperatures as other instruments used in the comparison. A likely source for at least some of the bias is the O densities, which are taken from the NRLMSISE-00 empirical atmospheric model [*Picone et al.*, 2002] for the SOFIE retrieval. For SABER, the O is measured by SABER itself and used in those temperature retrievals.

[33] A comparison of the OSIRIS O measurements derived from O_2 A-band measurements with those of the NRLMSISE-00 model suggests that NRLMSISE-00 concentrations are a factor of five to ten too low [*Sheese et al.*, 2011b] and that the seasonal oscillations of NRLMSISE-00 O are six months out of phase. Thus while the use of the NRLMSISE-00 model is illustrative of showing the effect of O on temperatures derived from CO_2, the use of model O may be a source of error in SOFIE temperature retrievals above 88 km.

[34] On the other hand, the SOFIE temperatures are reduced by only 7 K at 95 km using SABER O profiles for co-located SOFIE temperature scans. The SABER O concentrations are about a factor of two larger than the NRLMSISE-00 O concentrations used in the SOFIE retrievals for the Arctic summer. This either means that SABER derived O is too low or that other mechanisms may be responsible for the SOFIE warm temperature bias between 88 and 95 km.

[35] In summary, the SOFIE v1.2 temperatures are consistent with several independent data sets to within quoted uncertainties up to 88 km altitude. Above 88 km uncertainties in O and CO_2 concentrations affect the temperature retrievals

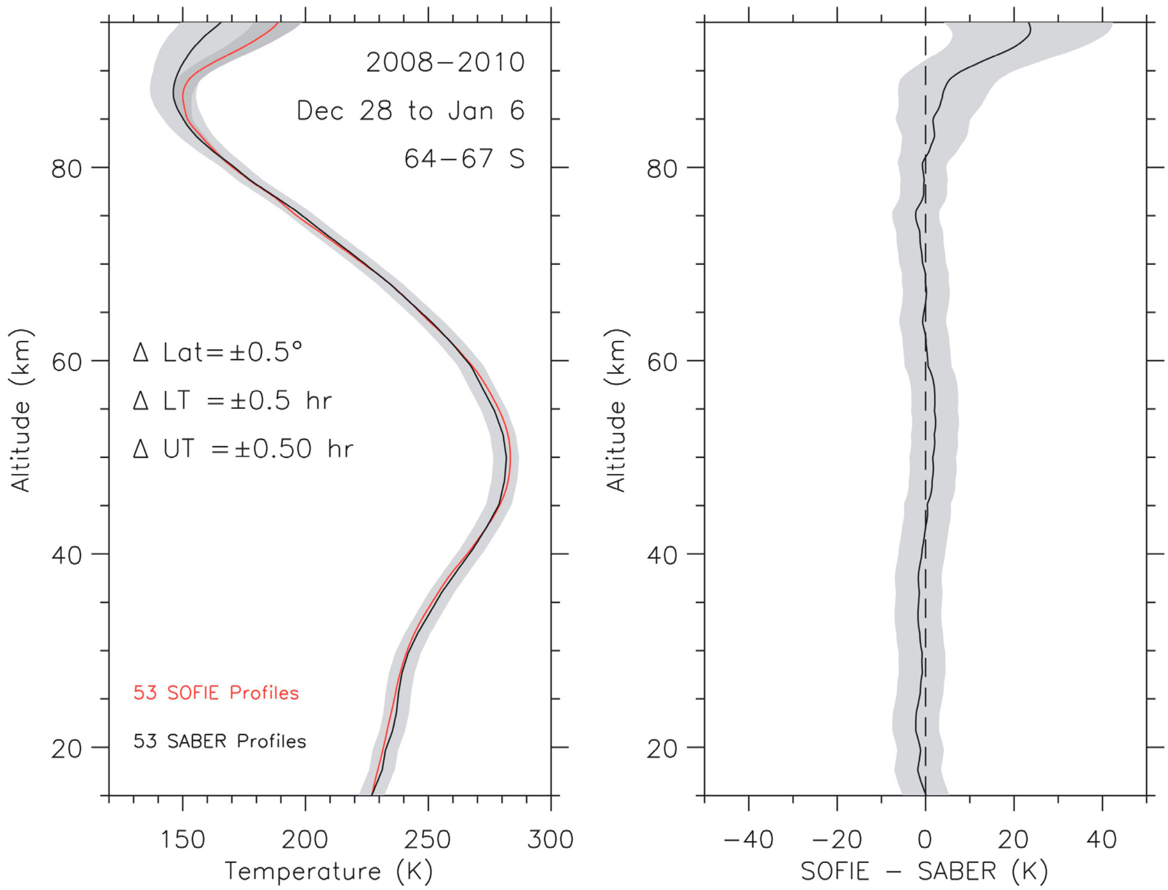

Figure 9. Comparisons with SABER temperatures as in Figure 4 but for the Antarctic summer. Constraints for finding SABER-SOFIE profiles are indicated as are the years, days and latitudes used.

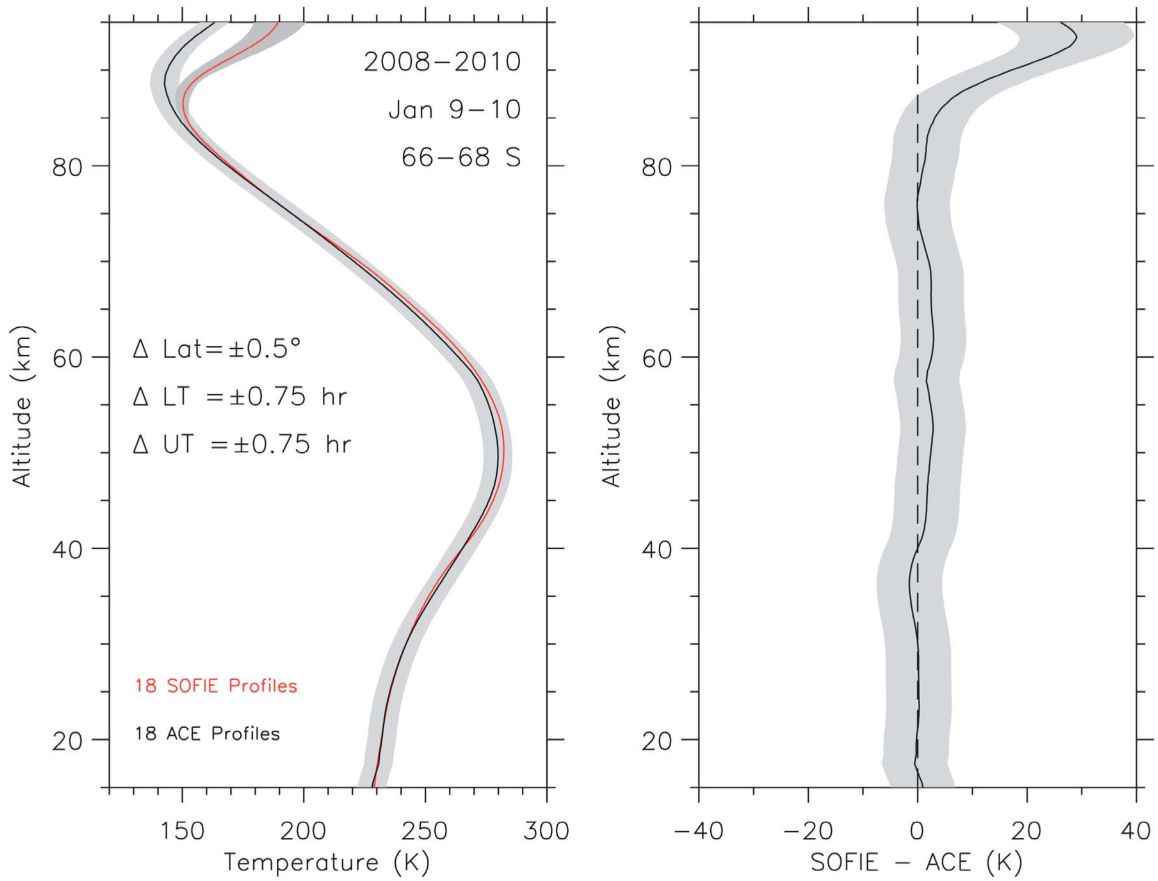

Figure 10. (left) Comparisons with ACE temperatures as in Figure 5 but for the Antarctic summer. The overplotted red curve shows the SOFIE profile smoothed over the 4 km vertical resolution of the ACE measurements. (right) The smoothed SOFIE profile is compared against the ACE average.

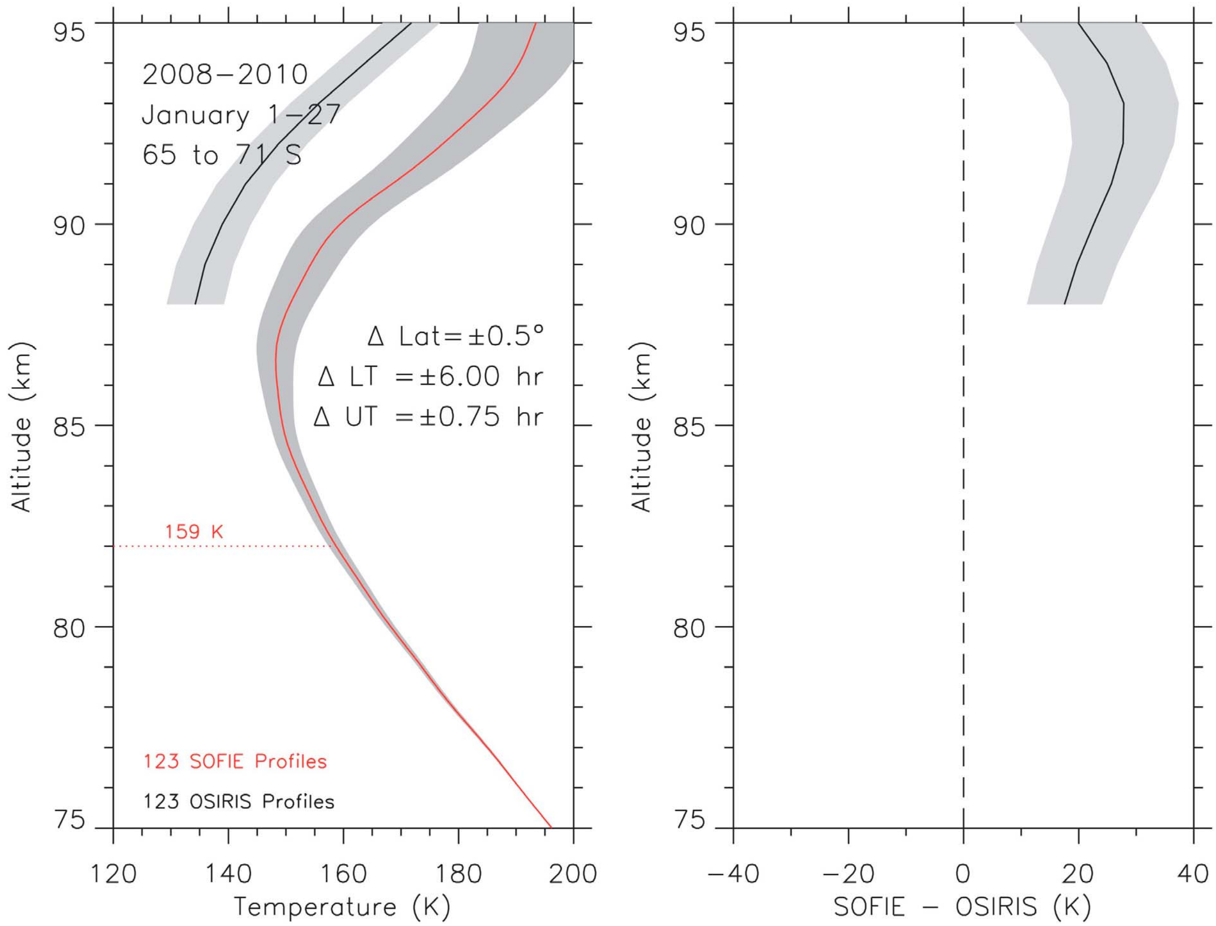

Figure 11. Comparisons with OSIRIS temperatures as in Figure 6 but for the Antarctic summer.

significantly, most likely leading to a warm bias in the SOFIE temperatures of 10–15 K in the Arctic summer and 20–30 K in the Antarctic summer. Further progress on the SOFIE temperature retrievals can be made when the local O and CO_2 concentrations between 88 and 95 km are better constrained.

[36] **Acknowledgments.** Funding of this research was provided by NASA's Small Explorers Program under contract NAS5–03132 that supports the implementation of the AIM mission. The Atmospheric Chemistry Experiment (ACE), also known as SCISAT, is a Canadian-led mission mainly supported by the Canadian Space Agency. We thank Andrew Kochenash for his assistance in the analysis of SABER temperatures.

References

Berger, U., and U. von Zahn (1999), The two-level structure of the mesopause: A model study, *J. Geophys. Res.*, *104*, 22,083–22,093, doi:10.1029/1999JD900389.

Garcia, R. R., D. R. Marsh, D. E. Kinnison, B. A. Boville, and F. Sassi (2007), Simulations of secular trends in the middle atmosphere, 1950–2003, *J. Geophys. Res.*, *112*, D09301, doi:10.1029/2006JD007485.

Gordley, L. L., et al. (2009), The solar occultation for ice experiment, *J. Atmos. Sol. Terr. Phys.*, *71*, 300–315, doi:10.1016/j.jastp.2008.07.012.

Hervig, M. E., and L. L. Gordley (2010), Temperature, shape, and phase of mesospheric ice from Solar Occultation for Ice Experiment observations, *J. Geophys. Res.*, *115*, D15208, doi:10.1029/2010JD013918.

Hervig, M. E., et al. (2009a), Relationships between polar mesospheric clouds, temperature, and water vapor from Solar Occultation for Ice Experiment (SOFIE) observations, *J. Geophys. Res.*, *114*, D20203, doi:10.1029/2009JD012302.

Hervig, M. E., L. L. Gordley, J. M. Russell III, and S. M. Bailey (2009b), SOFIE PMC observations during the northern summer of 2007, *J. Atmos. Sol. Terr. Phys.*, *71*, 331–339, doi:10.1016/j.jastp.2008.08.010.

Höffner, J., and F.-J. Lübken (2007), Potassium lidar temperatures and densities in the mesopause region at Spitsbergen (78°N), *J. Geophys. Res.*, *112*, D20114, doi:10.1029/2007JD008612.

Kutepov, A. A., et al. (2006), SABER temperature observations in the summer polar mesosphere and lower thermosphere: Importance of accounting for the CO_2 ν_2 quanta V–V exchange, *Geophys. Res. Lett.*, *33*, L21809, doi:10.1029/2006GL026591.

Lautenbach, J., and J. Höffner (2004), Scanning iron temperature lidar for mesopause temperature observation, *Appl. Opt.*, *43*, 4559–4563, doi:10.1364/AO.43.004559.

López-Puertas, M., and F. W. Taylor (2001), *Non-LTE Radiative Transfer in the Atmosphere*, World Sci., Singapore, doi:10.1142/9789812811493.

Lübken, F.-J. (1999), Thermal structure of the Arctic summer mesosphere, *J. Geophys. Res.*, *104*, 9135–9149.

Lübken, F.-J. (2000), Nearly zero temperature trend in the polar summer mesosphere, *Geophys. Res. Lett.*, *27*, 3603–3606, doi:10.1029/2000GL011893.

Lübken, F.-J., and A. Müllemann (2003), First in situ temperature measurements in the summer mesosphere at very high latitudes (78°N), *J. Geophys. Res.*, *108*(D8), 8448, doi:10.1029/2002JD002414.

Lübken, F.-J., K.-H. Fricke, and M. Langer (1996), Noctilucent clouds and the thermal structure near the Arctic mesopause in the summer, *J. Geophys. Res.*, *101*, 9489–9508, doi:10.1029/96JD00444.

Lübken, F.-J., A. Müllemann, and M. J. Jarvis (2004), Temperatures and horizontal winds in the Antarctic summer mesosphere, *J. Geophys. Res.*, *109*, D24112, doi:10.1029/2004JD005133.

Lübken, F.-J., J. Lautenbach, J. Höffner, M. Rapp, and M. Zecha (2009), First continuous temperature measurements within polar mesosphere summer echoes, *J. Atmos. Sol. Terr. Phys.*, *71*, 453–463, doi:10.1016/j.jastp.2008.06.001.

Marshall, B. T., et al. (2011), Retrieval of temperature and pressure using broadband solar occultation: SOFIE approach and results, *Atmos. Meas. Tech.*, *4*, 893–907, doi:10.5194/amt-4-893-2011.

Mertens, C. J., et al. (2001), Retrieval of mesospheric and lower thermospheric kinetic temperature from measurements of CO_2 15 μm Earth limb emission under non-LTE conditions, *Geophys. Res. Lett.*, *28*, 1391–1394, doi:10.1029/2000GL012189.

Petelina, S. V., and A. Y. Zasetsky (2009), Temperature of mesospheric ice retrieved from the O-H stretch band, *Geophys. Res. Lett.*, *36*, L15804, doi:10.1029/2009GL038488.

Picone, J. M., A. E. Hedin, D. P. Drob, and A. C. Aikin (2002), NRLMSISE-00 empirical model of the atmosphere: Statistical comparisons and scientific issues, *J. Geophys. Res.*, *107*(A12), 1468, doi:10.1029/2002JA009430.

Rapp, M., F.-J. Lübken, A. Mullemann, G. E. Thomas, and E. J. Jensen (2002), Small-scale temperature variations in the vicinity of NLC: Experimental and model results, *J. Geophys. Res.*, *107*(D19), 4392, doi:10.1029/2001JD001241.

Remsberg, E. E., et al. (2008), Assessment of the quality of the Version 1.07 temperature-versus-pressure profiles of the middle atmosphere from TIMED/SABER, *J. Geophys. Res.*, *113*, D17101, doi:10.1029/2008JD010013.

Russell, J. M., III, et al. (2009), The Aeronomy of Ice in the Mesosphere (AIM) mission: Overview and early science results, *J. Atmos. Sol. Terr. Phys.*, *71*, 289–299, doi:10.1016/j.jastp.2008.08.011.

Russell, J. M., III, P. Rong, S. M. Bailey, M. E. Hervig, and S. V. Petelina (2010), Relationship between the summer mesopause and polar mesospheric cloud heights, *J. Geophys. Res.*, *115*, D16209, doi:10.1029/2010JD013852.

Sheese, P. E., E. J. Llewellyn, R. L. Gattinger, A. E. Bourassa, D. A. Degenstein, N. D. Lloyd, and I. C. McDade (2011a), Mesopause temperatures during the polar mesospheric cloud season, *Geophys. Res. Lett.*, *38*, L11803, doi:10.1029/2011GL047437.

Sheese, P. E., I. C. McDade, R. L. Gattinger, and E. J. Llewellyn (2011b), Atomic oxygen densities retrieved from Optical Spectrograph and Infrared Imaging System observations of O_2 A-band airglow emission in the mesosphere and lower thermosphere, *J. Geophys. Res.*, *116*, D01303, doi:10.1029/2010JD014640.

Sica, R. J., et al. (2008), Validation of the Atmospheric Chemistry Experiment (ACE) version 2.2 temperature using ground-based and space-borne measurements, *Atmos. Chem. Phys.*, *8*, 35–62, doi:10.5194/acp-8-35-2008.

Siskind, D. E., et al. (2011), Consequences of recent Southern Hemisphere winter variability on polar mesospheric clouds, *J. Atmos. Sol. Terr. Phys.*, *73*, 2013–2021, doi:10.1016/j.jastp.2011.06.014.

Smith, A. K., D. R. Marsh, M. G. Mlynczak, and J. C. Mast (2010), Temporal variations of atomic oxygen in the upper mesosphere from SABER, *J. Geophys. Res.*, *115*, D18309, doi:10.1029/2009JD013434.

Theon, J. S., W. Nordberg, L. B. Katchen, and J. J. Horvath (1967), Some observations on the thermal behavior of the mesosphere, *J. Atmos. Sci.*, *24*, 428–438, doi:10.1175/1520-0469(1967)024<0428:SOOTTB>2.0.CO;2.

von Zahn, U., J. Höffner, V. Eska, and M. Alpers (1996), The mesopause altitude: Only two distinctive levels worldwide?, *Geophys. Res. Lett.*, *23*, 3231–3234, doi:10.1029/96GL03041.